Z. Phys. A – Atomic Nuclei 333, 271–279 (1989)

Zeitschrift für Physik A
Atomic Nuclei

Mechanism of Reactions Induced by 7 MeV Deuterons on ^{9}Be [(d, p), (d, d), (d, t), $(d, ^4\mathrm{He})$]

A. Szczurek*[1], K. Bodek*,[1], J. Krug[1], W. Lübcke[1], H. Rühl[1], M. Steinke[1], M. Stephan[1], D. Kamke[1], W. Hajdas[2], L. Jarczyk[2], B. Kamys[2], A. Strzałkowski[2], and E. Kwasniewicz[3]**

[1] Institut für Experimentalphysik I der Ruhr-Universität Bochum, Federal Republik of Germany
[2] Institute of Physics, Jagellonian University, Cracow, Poland
[3] Institute of Physics, Silesian Technical University, Katowice, Poland

Received November 21, 1988; revised version February 27, 1989

Angular distributions of protons, deuterons, tritons and alpha-particles emitted from the reactions in the $d + ^9$Be-system at $E_d = 7$ MeV as well as excitation functions at selected angles in the energy range $E_d = 6.5$–7.5 MeV (LAB) were measured. The potential part of the elastic scattering is described by the phenomenological optical model. The compound nucleus contribution to all exit channels is determined using the Hauser-Feshbach model. The collective excitation of the 2.43 MeV excited state of ^{9}Be and transfer processes are analysed within the DWBA formalism. The analyses suggest a significant contribution of five-nucleon transfer to the $(d, ^4\mathrm{He})$ channel.

Nuclear Reactions: ^{9}Be(d, p), ^{9}Be(d, d), ^{9}Be(d, t), ^{9}Be$(d, ^4\mathrm{He})$, measured: $\sigma(\Theta)$, $E_{\mathrm{lab}} = 7$ MeV, $\sigma(\Theta, E)$, $E_{\mathrm{lab}} = 6.5$–7.5 MeV, optical model, Hauser-Feshbach model and DWBA analysis.

PACS: 24.50.+g; 24.60.+m; 25.50.−n

1. Introduction

Nuclear reactions induced by deuterons on ^{9}Be are interesting due to specific properties of the interacting particles. Both the deuteron and the ^{9}Be nucleus are loosely bound: the neutron binding energy is 2.225 MeV for the deuteron and 1.665 MeV for ^{9}Be (g.s.). The energy for separating alpha-particles in ^{9}Be is also low (2.47 MeV). Furthermore, the spectroscopic factors of the neutron in both nuclei [1] as well as of the $^4\mathrm{He} + ^5\mathrm{He}$ partition of ^{9}Be are large [1, 2]. According to these features of the entrance channel one can expect that even at low energies some exit channels are strongly populated by direct reaction mechanism.

Reactions induced by deuterons on ^{9}Be have been the object of many investigations in the past:

– *Elastic scattering* was measured and analysed by Lombaard et al. [3] at 1.1–2.2 MeV, Zwieglinsky et al. [4] at 1.1–2.5 MeV, Powell et al. [5] at 4.5–6 MeV, Djaloeis et al. [6] at 5–7 MeV, Green and Parkinson [7] at 7.8 MeV, and by Fitz et al. [8] at 11.8 MeV. The experimental data were analysed in terms of a phenomenological optical model supplemented in some cases by compound nucleus contributions.

– *Inelastic scattering* leading to the 2.43 MeV $(5/2^-)$ state of ^{9}Be was measured by Fitz et al. [8] at 11.8 MeV and analysed within the DWBA. These calculations were performed, however, in an approximate way and the absolute value of the cross section was fitted to the experimental data.

– The $^9Be(d, p)^{10}Be$ reaction was studied by Friedland et al. [9] at 0.6–2.7 MeV, Zwieglinski et al. [10] at 0.9–3.1 MeV, Fulbright et al. [11] at 3.6 MeV, Powell et al. [5] at 4.55 MeV, by Green and Parkinson [7] at 7.8 MeV, Griffith et al. [12] at 11.8 MeV, Schiffer et al. [13] at 12 MeV, Darden et al. [14] at 15 MeV, and by Anderson et al. [15] at 17.3 MeV.

– The $^9Be(d, t)^8Be$ reaction was the object of investigations by Biggerstaff et al. [16] at 0.4–2.4 MeV,

* On leave from the Jagellonian University, Cracow, Poland
** Alexander-von-Humboldt fellow

Friedland et al. [9] at 0.6–2.7 MeV, Zwieglinski et al. [10] at 0.9–3.1 MeV, Fulbright et al. [11] at 3.6 MeV, Fitz et al. [8] at 11.8 MeV, and of Tanaka [17] at 12.17 MeV and 14.43 MeV. Angular distributions for both the (d, p) and (d, t) reactions were analysed by means of either the zero-range or no-recoil DWBA. Spectroscopic factors obtained from fits to the experimental data, however, were different for different beam energies.

– The $^{9}Be(d, ^{4}He)^{7}Li$ reaction was investigated by Friedland et al. [9] at 0.6–2.7 MeV, Sledzinska et al. [18] at 0.9–3.1 MeV, Biggerstaff et al. [16] at 2.25–3.1 MeV, Tanaka [17] at 12.17 MeV and 14.43 MeV, Yanabu et al. [19] at 14.5 MeV, and by Mayo et al. [20] at 27 MeV. In [18, 20] a deuteron transfer was claimed to be the dominant process whereas in [17] it was compound nucleus mechanism. A ^{5}He transfer was taken into account in [17] in the zero-range DWBA with a limited number of orbitals in ^{9}Be and ^{7}Li. There are also indications that this process plays an important role in the similar reactions $^{12}C(^{9}Be, \alpha)^{17}O$ and $^{12}C(d, ^{7}Li)^{7}Be$ [21, 22].

The *aim of the present work* was to find the mechanism of the reactions in the $d + ^{9}$Be system by a simultaneous study of several outgoing channels. Angular distributions were measured for different states of the residual nuclei for the $p, d, t, ^{4}$He outgoing channels. Additionally the measurement of excitation functions was performed to check whether the chosen energy region is free of conspicuous structures. Different processes like potential scattering, compound nucleus mechanism, transfer reactions and collective excitation were taken into account in the analysis of the experimental data. Whenever possible the parameters were given the commonly accepted values (e.g. geometrical parameters of bound state potentials) which were then no longer taken as free fitting parameters.

The spectroscopic amplitudes were calculated in the frame of the shell model. In an attempt to obtain as much consistency as possible the same optical potentials were used to generate the distorted wave functions for the DWBA model, the transmission coefficients for the Hauser-Feshbach model, the inelastic form factor, and also for the description of elastic scattering. The exact finite-range DWBA was used to describe the direct reactions.

2. Experiment

The experiments were performed at the Dynamitron-Tandem Laboratory of the Ruhr-University in Bochum. A pulsed deuteron beam (pulse FWHM 0.8 ns, repetition period 200 ns) of 7 MeV energy and with the (average) current of 10–20 nA was focussed onto a 2 mm diameter spot on the target placed in the center of a 60 cm ⌀ scattering chamber. A self-supporting ^{9}Be foil (thickness of about 50 μg/cm^2) was used as the target. The energy vs. time-of-flight (E-TOF) and the $\Delta E - E$ method were applied for particle identification. Five silicon surface-barrier detectors, each 1 mm thick with a solid angle of 0.91 msr placed 235 mm from the target, detected particles by the E-TOF method. The flight-times were measured between fast signals delivered by the detectors and the buncher. The total time resolution (FWHM) was about 3 ns allowing good separation of the p, d, t and alpha-particles in the whole energy range except at the highest energies of the hydrogen isotopes. In order to separate the p, d and t ejectiles one $\Delta E - E$ silicon counter telescope (39.5 μm and 1000 μm) with a solid angle of 0.89 msr was used. The total energy resolution, mainly due to kinematical broadening and target thickness, was below 80 keV for protons and 150 keV for alpha-particles.

For the angular distributions the spectra of the emitted particles were measured in the angular range between 30° and 170° (LAB) in steps of 5°. Typical examples of spectra are presented in Fig. 1.

The absolute cross-section was obtained by referring to the elastic scattering cross-section of deuterons from ^{9}Be, which, on its own part, was obtained by referring it to the Rutherford scattering from a gold layer of known thickness evaporated on the target.

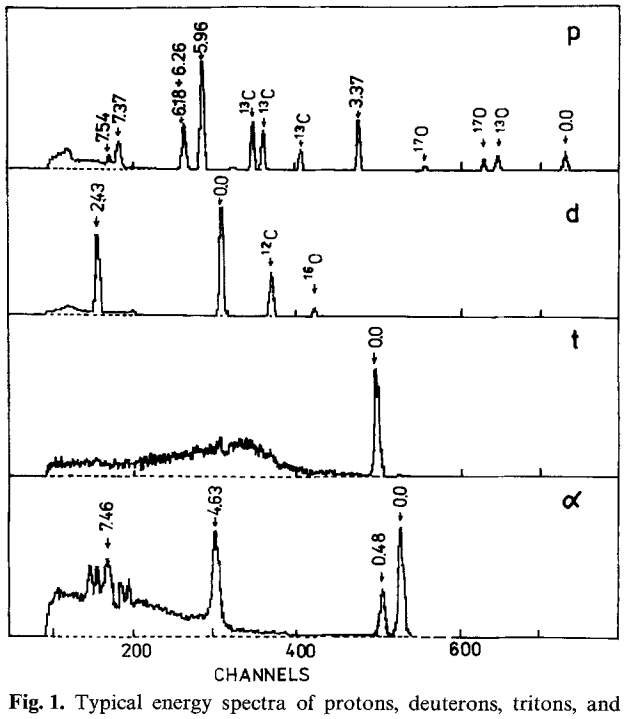

Fig. 1. Typical energy spectra of protons, deuterons, tritons, and α-particles at $\Theta_{lab} = 125°$. The peaks are labeled with the excitation energies of the corresponding nuclear states

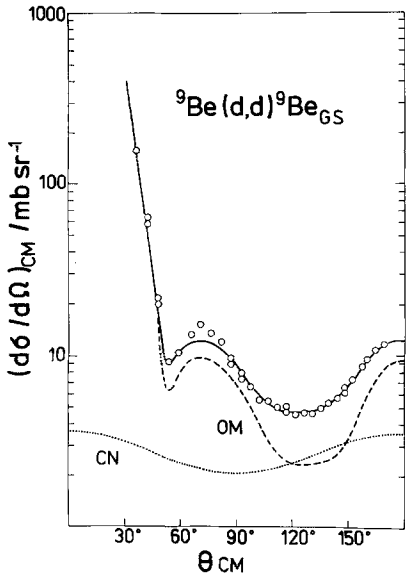

Fig. 2. Experimental angular distribution (circles) for the elastic scattering of 7.0 MeV deuterons from ^{9}Be compared with calculations. The optical model contribution is represented by the dashed, the compound nucleus contribution by the dotted line. The solid line represents the incoherent sum of these two cross sections

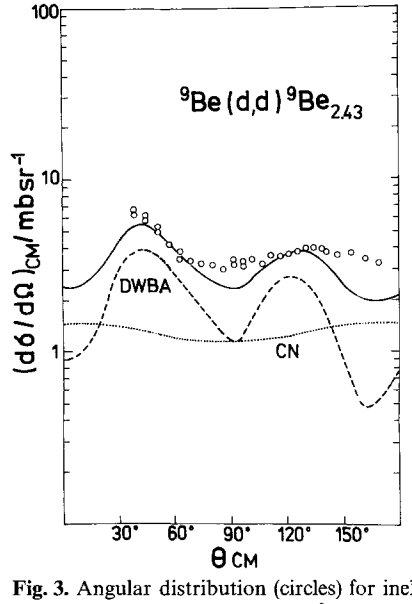

Fig. 3. Angular distribution (circles) for inelastic scattering leading to the 2.43 MeV (5/2$^-$) state of ^{9}Be, E_d=7.0 MeV. The collective excitation contribution is shown by the dashed, the compound nucleus contribution by the dotted line. The solid line represents the incoherent sum of these two cross sections

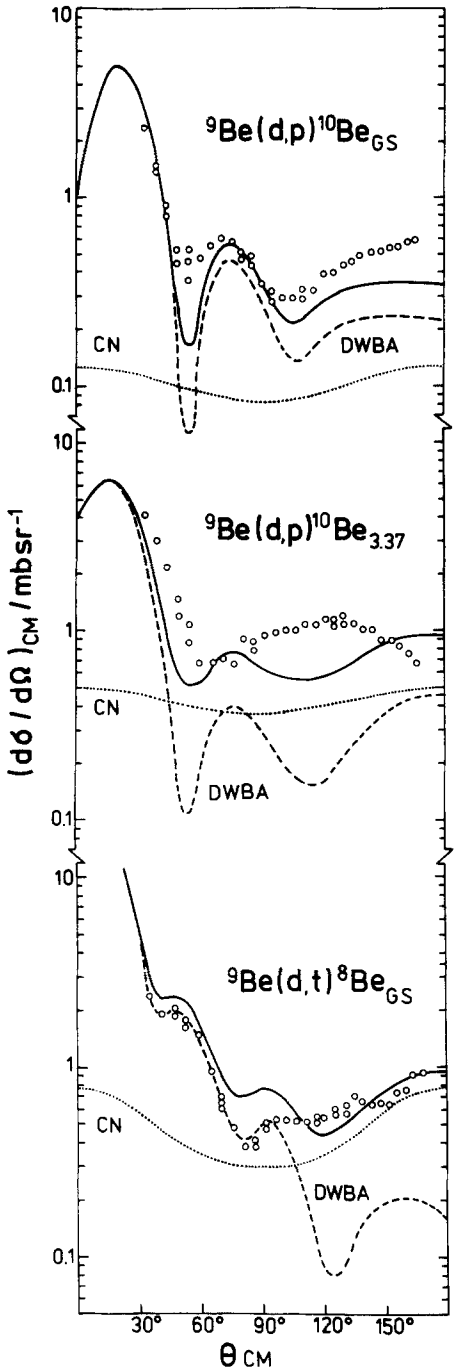

Fig. 4. Angular distributions (circles) for the p_0, p_1 and t_0 channels at 7.0 MeV. The dashed curves represent the transfer, the dotted lines the compound nucleus contributions. The solid line represents the incoherent sum of these two cross sections

Dead times were corrected for. The relative statistical errors of the individual points are 3–6% whereas an overall uncertainty in the absolute normalization was estimated to 8%. Experimental angular distributions are presented in Figs. 2–5.

Excitation functions in the energy range from 6.5 to 7.5 MeV were measured in 100 keV steps for the LAB-angles Θ=40°, 100°, 140°, 150°, 160°, and 170°, with typical examples being shown in Fig. 6.

Table 1 contains a list of the states of the residual nuclei investigated in this experiment together with their known excitation energies and spin/parity assignments.

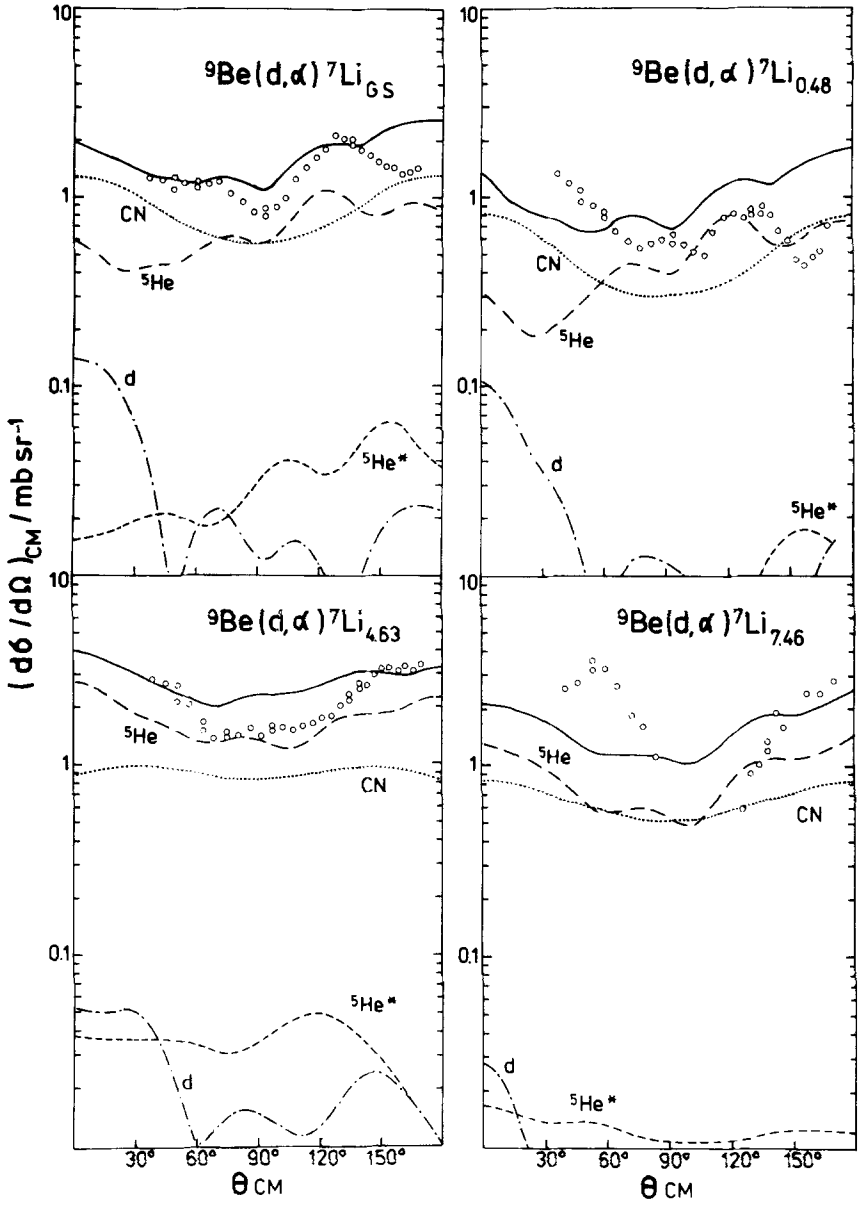

Fig. 5. Contributions of different reaction processes for the α_0, α_1, α_2, and α_3 channels. The long-dashed curves gives the $^5He_{gs}$ transfer, short-dashed: $^5He^*$ transfer, dash-dotted: deuteron transfer, dotted: compound nucleus contribution, and the solid line the incoherent sum of all these processes

3. Elastic Scattering

The elastic scattering can mainly be described by an average potential interaction. For light nuclear systems at low energies, however, the compound nucleus contribution to the elastic scattering has to be taken into account [5, 27]. In order to generate the transmission coefficients for the Hauser-Feshbach model calculations the parameters for the optical potential were initially taken from fits to the elastic scattering data. Later on a self-consistent search was performed, including compound nucleus formation and the incoherent potential contribution to the elastic scattering. The compound nucleus cross section was calculated by the Hauser-Feshbach model according to the procedure in Chap. 4. The six-parameter optical model potential

$$V(r) = U * f_u(r) + iW * f_w(r) + V_c(r)$$

with Woods-Saxon form factors

$$f_1(r) = 1/(1 + \exp((r - r_i A^{1/3})/a))$$

was used in the analysis. The nuclear potential is supplemented by the Coulomb-Potential $V_c(r)$ of a uniform charge distribution of radius $R = 1.3\, A^{1/3}$ fm. The computer code SCAT [23] was applied in the numerical calculations.

The search for parameters was performed while keeping U between 40 and 200 MeV. The resulting

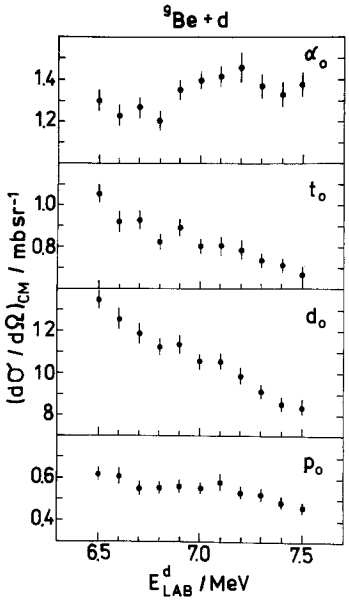

Fig. 6. Experimental excitation functions of the ^{9}Be(d, p), ^{9}Be(d, d), ^{9}Be(d, t), and ^{9}Be($d, ^4$He) reactions in the energy range from 6.5 to 7.5 MeV, taken at $\Theta_{lab} = 160°$

Table 1. Data of the states of the residual nuclei investigated

Exit channel	Excitation energy [MeV] (spin, parity)
1. $p + ^{10}$Be	0.0 (0^+) 3.37 (2^+)
2. $d + ^9$Be	0.00 ($3/2^-$) 2.43 ($5/2^-$)
3. $t + ^8$Be	0.00 (0^+)
4. ^{4}He + ^{7}Li	0.00 ($3/2^-$) 0.48 ($1/2^-$) 4.63 ($7/2^-$) 7.46 ($5/2^-$)

families of the optical model potentials equivalent in the quality of the overall fit are listed in Table 2. In the further steps of the analysis including also inelastic scattering and transfer reactions (Chaps. 5 and 6, respectively) the potential listed at position 2 of Table 2 was singled out as giving the best and most consistent description of *all* measured reaction channels. This potential has a rather small radius and large diffuseness of the real part as a consequence of the extended structure of the deuteron, according to Satchler's folding optical model studies [24].

4. Compound Nucleus Contributions

The energy $E_d = 7$ MeV of the incoming deuterons leads to the excitation energy 21.5 MeV of the compound nucleus ^{11}B. At this energy the density of states in the compound nucleus is fairly high: 100–200 states per MeV according to the formula of Gilbert and Cameron [25]. Therefore the observation of isolated resonances is improbable. In accordance the measured excitation curves (Fig. 6) do not show any conspucious structures, and it seemed appropriate to apply the Hauser-Feshbach formula [26] in order to determine the energy-averaged compound nucleus contributions. The c.m. differential cross-section is given by

$$\frac{\mathrm{d}\,\sigma_{cc'}(\Theta_{CM})}{\mathrm{d}\,\Omega_{CM}} = \frac{R(1+\delta_{cc'})}{4k^2(2I_A+1)(2I_a+1)} \sum_{L,J,\pi} \sum_{s,l} T_l^c \sum_{s';l'} (-1)^{s-s'} \cdot \frac{T_{l'}^{c'}}{\sum_{c'',l''} T_{l''}^{c''}} Z(l,J,l,J;s,L)\, Z(l',J,l',J;s',L) \cdot P_L(\cos\theta_{CM}), \quad (1)$$

with

$$\sum_{c'',l''} T_{l''}^{c''} := \sum_{\substack{c'',l'' \\ E<E_{c''}}} T_{l''}^{c''} + \sum_{c'',l''} \int_{E_{c''}}^{E^{c''}_{\max}} \rho(E)\, T_{l''}^{c''}\, \mathrm{d}\,E,$$

and where I_A, I_a are spins of the incoming particles, J, π spin and parity of the compound state, s the channel spin and l, l', l'', orbital angular momenta, $E_{c''}$ the maximum energy of the discrete levels, and $E^{c''}_{\max}$ is the maximum available energy of the residual nuclei in channel c''. The symbols T_l^c denote usual transmission coefficients. Compound elastic enhancement is accounted for by the factor $(1+\delta_{cc'})$. The function $\rho(E)$ stands for the density-of-states of the residual nuclei in channel c''. According to Hodgson and Wilmore [27] the cross-section formula (1) assumes that all partial waves in channel c contribute to the formation of the compound nucleus; the presence of non-compound nuclear reactions, i.e. by excitation of direct modes, is taken into account by reducing the cross-sections for the different exit channels c' by a factor R, common to *all* channels (including elastic, inelastic and rearrangement channels). The summation in the denominator of (1) was performed over all known discrete levels [28, 29] while in the region of overlapping levels the level-density formula of Gilbert and Cameron [25] was used. The spin-cutoff parameter and the pairing-energy were calculated following the same paper. For the level density parameter a we took $a = A/C$ with $C = 5$ [30] and A being the mass number of the nucleus under consideration. Changing C by a factor of two changes the cross-

Table 2. Sets of optical model parameters for elatic scattering of deuterons from ^{9}Be at 7 MeV

	U [MeV]	r_u [fm]	a_u [fm]	W [MeV]	r_w [fm]	a_w [fm]	number of nodes	volume integral	χ^2
1.	50.0	1.127	0.901	5.76	2.07	1.05	2	358	21.8
2.	150.0	0.864	1.100	12.79	2.19	0.334	3	969	13.4
3.	140.0	0.959	0.884	15.2	1.47	0.960	3	743	35.8
4.	182.0	1.234	0.939	13.9	2.40	0.172	4	1616	35.0

Table 3. Characteristics of channels taken into account in the Hauser-Feshbach analysis at 7 MeV

Channel	Q-value [MeV]	Maximum excitation energy of residual nucleus [MeV]	Maximum energy of discrete levels included in the analysis [MeV]
1. $n+^{10}$B	4.3607	10.09	8.7
2. $p+^{10}$Be	4.5874	10.31	9.4
3. $d+^{9}$Be	0.0	5.73	5.73
4. $t+^{8}$Be	4.5925	10.32	10.32
5. ^{4}He+^{7}Li	7.1512	12.88	12.88
6. ^{5}He+^{6}Li	−0.9928	4.73	4.73

section less than 10% due to the dominant participation of discrete levels in the denominator of (1). The channels taken into account in these calculations are presented in Table 3, whereas the parameters for the optical potentials used in order to find the transmission coefficients are listed in Table 4. The calculations were performed using the code STATIS of Stokstad [35].

The only remaining free parameter is the reduction factor R. Its value was adjusted b requiring that the calculated compound nucleus cross-section for each outgoing channel must not exceed the experimental cross-section. By this method a maximum value of $R=0.21$ was found. It is close to the values obtained for ^{9}Be$(d,p)^{10}$Be [5], ^{12}C$(d,d)^{12}$C [36], and ^{23}Na$(p,p)^{23}$Na [37] in a similar energy range; we mention this without further discussion. The compound nucleus cross-sections for different exit channels are depicted in Figs. 3–5.

5. Inelastic Scattering

Calculations of the inelastic cross-sections leading to the 2.43 MeV ($5/2^-$) state of ^{9}Be were performed by means of the DWBA, assuming rotational collective excitation [38]. The computer code JUPITER 4 was used [39]. Distorted wave functions followed from the optical model potential No. 2, Table 2. Both real and imaginary coupling were included in the analysis. The results of the calculations showed that Coulomb-excitation is negligible. The deformation length βR was adjusted to reproduce the experimental data including the compound nucleus contribution obtained as described in Chap. 4. The results of the DWBA calculation, the compound nucleus contribution as well as the incoherent sum of these processes, are shown in Fig. 3. The positions of the maxima of the experimental angular distributions are reproduced fairly well by the DWBA. The compound nucleus contribution flattens the sharp oscillations given by the DWBA. As this damping is consistent with the experimental data it may provide further evidence for the presence of compound nucleus mechanism. The value of the deformation length found in the present analysis is $|\beta R|=3.7$ fm. It is larger than those obtained by Harakeh et al. [40] ($|\beta R|=1.80$ fm) for ^{9}Be(α,α), Votava et al. [41] (2.63 fm), and by Satchler [42] (2.9 fm) for the ^{9}Be(p,p) reactions. If $R(^9\text{Be})=1.1\,A^{1/3}$ fm is accepted, the big value of βR is consistent with values of the intrinsic quadrupole moment [43] and with the value for $B(E2)$ [44].

6. Transfer Reactions

The transfer reactions were analysed within the exact finite-range Born approximation using the SATURN-MARS code of Tamura and Low [45]. The distorted waves in the entrance and exit channels were generated by means of the optical model with the potential parameters listed in Table 4. The bound state wave functions were calculated using the Woods-Saxon potential with depth adjusted to reproduce the binding energies. The commonly accepted geometrical parameters $R=1.25\,A^{1/3}$ fm and $a=0.65$ fm were used for the neutron binding potentials in ^{9}Be and ^{10}Be, whereas $R=0.85*(A_1^{1/3}+A_2^{1/3})$ fm and $a=0.65$ fm were chosen for the heavier clusters because these values gave a consistent description for the transfer reactions in the similar systems ^{10}B$+\alpha$, ^{11}B$+^3$He and ^{12}C$+d$ [22, 46, 47, 48].

According to the well known DWBA equivalence of prior- and post-representations [49] the transition

Table 4. Optical model parameters in the Hauser-Feshbach and DWBA analyses

Channel	U [MeV]	r_u [fm]	a_u [fm]	W_v [MeV]	r_v [fm]	a_v [fm]	W_s [MeV]	r_s [fm]	a_s [fm]	r_c [fm]	Ref.
$n+^{10}B$	45.6	1.31	0.66	–	–	–	9.08	1.26	0.48	–	[31]
$p+^{10}Be$	45.6	1.31	0.66	–	–	–	9.08	1.26	0.48	1.3	[31]
$d+^{9}Be$	150.0	0.864	1.100	12.79	2.19	0.334	–	–	–	1.3	[a]
$t+^{8}Be$	141.2	1.156	0.758	16.4	1.535	0.990	–	–	–	1.07	[32]
$^{4}He+^{7}Li$	149.2	1.736	0.56	–	–	–	9.1	1.736	0.56	1.736	[33]
$^{5}He+^{6}Li$	72.63	1.36	0.765	23.8	1.34	0.765	–	–	–	1.3	[34]

[a] Present work

Table 5. Bound-state characteristics for the neutron transfer reactions

Nucleus	Core	Cluster	n	l	j	Spectr. ampl.	Other Refs.	Binding energy [MeV]
$^{10}Be\ 0.0(0^+)$	^{9}Be	n	0	1	3/2	1.535	[8, 9, 14, 17], [1]	6.812
$^{10}Be\ 3.37(2^+)$	^{9}Be	n	0	1	1/2	0.461		3.444
			0	1	3/2	−0.232		
d	p	n	0	0	1/2	1.421		2.225
^{9}Be	$^{8}Be(0^+)$	n	0	1	3/2	0.762	[5, 9, 10, 13, 15], [1]	1.665
t	d	n	0	0	1/2	1.225		6.258

potential can be defined in the following two forms (for stripping of a "t"-cluster):

$V_{C_1,t}+V_{C_1,C_2}-U^{\text{o.m.}}_{C_2,C_1}+t$ for the initial $(C_1+t)+C_2-$,
and

$V_{C_1,t}+V_{C_2,C_1}-U^{\text{o.m.}}_{C_1,C_2}+t$ for the final $C_1+(C_2+t)-$

fragmentation, leading to the same (on-shell) cross-section. This does not hold longer, if, to a further standard approximation, the core-core-potentials $V_{C_1,C_2}=V_{C_2,C_1}$ (which are not so well defined) are assumed to cancel the optical model potentials $U^{\text{o.m.}}_{C_2,C_1}$ and $U^{\text{o.m.}}_{C_1,C_2}$, respectively. In order to be physically consistent one then has to decide in each case which representation gives the best cancellation. We followed this frequently used procedure and decided to take the prior-representation for the (d,t)- and (d,α)-reactions, and the post-representation for the (d,p)-reactions.

The required spectroscopic amplitudes were obtained from intermediate-coupling shell-model calculations. Thus the calculations were performed virtually without free parameters. The compound nucleus contribution, obtained according to Chap. 4, was included in all cases.

A. Neutron Transfer

Neutron stripping and pickup were assumed as the direct processes leading to p and t outgoing channels, respectively. The results of the calculations for the (d,p_0), (d,p_1) and (d,t_0) reactions are given in Fig. 4. These calculations were performed using spectroscopic amplitudes listed in Table 5. It is apparent that the cross sections are well reproduced in terms of the DWBA theory only for forward angles, whereas at backward angles the compound nucleus contribution is significant and dominant for the (d,t_0) reaction. It should be pointed out that an appropriate description of the data could be obtained only by using the deuteron optical potential no. 2 (Table 2) while the other families of potentials therein did not reproduce all experimental data consistently.

B. $^{9}Be(d,^{4}He)^{7}Li$ Reaction

The calculations of the compound nucleus contribution for the $^{9}Be(d,^{4}He)^{7}Li$ reaction (see Fig. 5) underestimate the cross section when compared to the experimental data. Furthermore, the latter show a diffractional pattern which cannot be reproduced in terms of the Hauser-Feshbach model. Therefore the deuteron transfer cross-sections were calculated for the measured alpha-channels. All parameters concerning the deuteron orbitals in the α-particle and in ^{7}Li are listed in Table 6. Results of the calculations are presented in Fig. 5. It is apparent that the sum of the compound nucleus contribution and the deute-

Table 6. Bound-state characteristics for the deuteron transfer reactions

Nucleus	Core	Cluster	n	l	j	Spectroscopic amplitude	Binding energy [MeV]
^{9}Be	^{7}Li	d	1	0	1	−0.155	16.697
	0.0(3/2$^-$)		0	2	1	−0.180	
			0	2	2	−0.100	
			0	2	3	0.558	
^{9}Be	^{7}Li	d	1	0	1	−0.252	17.174
	0.48(1/2$^-$)		0	2	1	0.174	
			0	2	2	−0.323	
^{9}Be	^{7}Li	d	0	2	2	−0.080	21.327
	4.63(7/2$^-$)		0	2	3	0.709	
^{9}Be	^{7}Li	d	1	0	1	0.712	24.156
	7.46(5/2$^-$)		0	2	1	−0.039	
			0	2	2	0.015	
			0	2	3	−0.520	
^{4}He	d	d	0	0	1	1.732	23.848

Table 7. Bound-state characteristics for the ^{5}He$_{gs}$ and ^{5}He* transfer reactions

Nucleus	Core	Cluster	n	l	j	Spectroscopic amplitude	Binding energy [MeV]
^{7}Li	d	^{5}He	1	0	3/2	−0.690	9.618
0.0(3/2$^-$)		(3/2$^-$)	0	2	1/2	−0.619	
			0	2	3/2	−0.402	
			0	2	5/2	−0.040	
^{7}Li	d	^{5}He	1	0	3/2	−0.881	9.140
0.48(1/2$^-$)		(3/2$^-$)	0	2	1/2	−0.226	
			0	2	3/2	−0.551	
^{7}Li	d	^{5}He	0	2	5/2	0.687	4.988
4.63(7/2$^-$)		(3/2$^-$)	0	2	7/2	0.768	
^{7}Li	d	^{5}He	1	0	3/2	0.702	2.158
7.46(5/2$^-$)		(3/2$^-$)	0	2	3/2	−0.554	
			0	2	5/2	−0.433	
			0	2	7/2	−0.314	
^{9}Be	^{4}He	^{5}He	2	0	3/2	0.750	2.467
		(3/2$^-$)	1	2	3/2	−0.744	
^{7}Li	d	^{5}He	1	0	1/2	−0.523	13.618
0.0(3/2$^-$)		(1/2$^-$)	0	2	3/2	0.410	
			0	2	5/2	0.020	
^{7}Li	d	^{5}He	1	0	1/2	−0.337	13.140
0.48(1/2$^-$)		(1/2$^-$)	0	2	3/2	0.464	
^{7}Li	d	^{5}He	0	2	5/2	0.639	8.988
4.63(7/2$^-$)		(1/2$^-$)					
^{7}Li	d	^{5}He	0	2	3/2	0.555	6.158
7.46(5/2$^-$)		(1/2$^-$)	0	2	5/2	0.033	
^{9}Be	^{4}He	^{5}He	1	2	3/2	0.248	6.467
		(1/2$^-$)					

ron transfer cross-section does not reproduce the experimental data. Since the transfer of five nucleons from ^{9}Be to the deuteron is another possible reaction mechanism leading to the same exit channel, this contribution was calculated in the cluster approximation assuming the pick-up of ^{5}He in its ground or first excited state. This procedure is intended only to give a simple prescription for calculating; it is not excluded that a second order (sequential) transfer of a neutron and an α-particle plays an important role. The quantum numbers of the transferred clusters, spectroscopic amplitudes and of the bound state parameters are given in Table 7. The sum of all coherent transfer processes and of the incoherent compound nucleus contribution are shown together with the experimental angular distributions in Fig. 5. The inclusion of the ^{5}He cluster transfer improves the description of the experimental angular distributions.

7. Conclusions

Contributions of different reaction mechanisms have been found for different exit channels in a combined analysis of our experimental data of the $d + ^9$Be-system at 7 MeV. The analysis shows that the contribution of the compound nucleus mechanism is about 20% making up a significant part of the cross-section mainly at backward angles in the (d, d), (d, p) and (d, t) channels (Fig. 4). Several families of optical model potentials for the $d + ^9$Be channel have been found when the contribution of the compound nucleus mechanism is included. By taking into account inelastic excitation and transfer reactions (only) *one* optical model potential family survives. The direct mechanism dominates as a neutron stripping for the (d, p)- and as a neutron pick-up for the (d, t)-reactions at forward angles. In the $(d, ^4$He) channels, see Fig. 5, the deuteron transfer gives only a small contribution, while a relatively large contribution of ^{5}He transfer was found in contrast to results in a previously published paper [17]. This demonstrates that the specific structure of the ^{9}Be nucleus as a weekly bound system of two alpha particles and a neutron strongly favors the five-nucleon transfer compared to deuteron transfer.

We thank the people being responsible for running the Dynamitron Tandem Laboratory of the Bochum University for technical help during the experiment. This work was partially supported by the Polish Central Research Program CPBP-01.06 No 12.4.

References

1. Cohen, S., Kurath, D.: Nucl. Phys. A**101**, 1 (1967)
2. Kwasniewicz, E., Jarczyk, L.: Nucl. Phys. A**441**, 77 (1985)
3. Lombaard, J.M., Friedland, E.: Z. Phys. **249**, 349 (1972)
4. Zwieglinski, B., Piotrowski, J., Saganek, A., Sledzinska, I.: Nucl. Phys. A**209**, 348 (1973)

5. Powell, D.L., Crawlay, G.M., Rao, B.V.N., Robson, B.A.: Nucl. Phys. A**147**, 65 (1970)
6. Djaloeis, A., Cords, H., Nurzynski, J.: Nucl. Phys. A**163**, 131 (1971)
7. Green, J.A., Parkinson, W.C.: Phys. Rev. **127**, 926 (1962)
8. Fitz, W., Jahr, R., Santo, R.: Nucl. Phys. A**101**, 449 (1967)
9. Friedland, E., Alberts, H.W., Staden, J.C. van: Z. Phys. **267**, 97 (1974)
10. Zwieglinski, B., Saganek, A., Sledzinska, I., Wilhelmi, Z.: Nucl. Phys. A**250**, 93 (1975)
11. Fulbright, H.W., Bruner, J.A., Bromley, D.A., Goldman, L.M.: Phys. Rev. **88**, 700 (1952)
12. Griffith, J.A.R., Irshad, M., Karban, D., Oh, S.W., Roman, S.: Nucl. Phys. A**167**, 87 (1971)
13. Schiffer, J.P., Morrison, G.C., Siemssen, R.H., Zeidman, B.: Phys. Rev. **164**, 1274 (1967)
14. Darden, S.E., Murillo, G., Sen, S.: Nucl. Phys. A**266**, 29 (1976)
15. Anderson, R.E., Kraushaar, J.J., Rickey, M.E., Zimmerman, W.R.: Nucl. Phys. A**236**, 77 (1974)
16. Biggerstaff, J.A., Hood, R.F., Scott, H., McEllistrem, M.T.: Nucl. Phys. **36**, 631 (1962)
17. Tanaka, S.: J. Phys. Soc. Japan **44**, 1405 (1978)
18. Sledzinska, I., Saganek, A., Wilhelmi, Z., Zwieglinski, B.: Acta. Phys. Pol. B**2**, 227 (1977)
19. Yanabu, T., Yamashita, S., Kakigi, S., Nguyen, D.C., Takimoto, K., Yamada, Y., Ogino, K.: J. Phys. Soc. Japan **19**, 1818 (1964)
20. Mayo, S., Testoni, J., Bilaniuk, O.M.: Phys. Rev. **133**, 350 (1964)
21. Jarczyk, L., Kamys, B., Okolowicz, J., Sromicki, J., Strzałkowski, A., Witała, H., Wrobel, Z., Hugi, M., Lang, J., Müller, R., Ungricht, E.: Nucl. Phys. A**325**, 510 (1979)
22. Jarczyk, L., Kamys, B., Rudy, Z., Strzałkowski, A., Styczen, B., Berg, G.P.A., Magiera, A., Meissburger, J., Oelert, W., Rossen, P. von, Römer, J.G.M., Tain, J.L., Wolter, H.H., Kwasniewicz, E., Kisiel, J.: Phys. Rev. C**33**, 934 (1986)
23. Smith, W.R.: Comput. Phys. Commun. **1**, 198 (1969)
24. Satchler, G.R.: Nucl. Phys. **85**, 273 (1966)
25. Gilbert, A., Cameron, A.G.W.: Can. J. Phys. **43**, 1446 (1965)
26. Hauser, W., Feshbach, H.: Phys. Rev. **87**, 366 (1952)
27. Hodgson, P.E., Wilmore, D.: Proc. Phys. Soc. **90**, 361 (1967)
28. Ajzenberg-Selove, F.: Nucl. Phys. A**320**, 1 (1979)
29. Ajzenberg-Selove, F.: Nucl. Phys. A**413/414**, 1 (1984)
30. Jarczyk, L., Kamys, B., Magiera, A., Strzałkowski, A., Szczurek, A., Bodek, K., Hugi, M., Lang, J., Müller, R., Ungricht, E.: J. Phys. **11**, 843 (1985)
31. Cookson, J.A., Locke, J.G.: Nucl. Phys. A**146**, 417 (1970)
32. Earwaker, L.G.: Nucl. Phys. A**90**, 56 (1967)
33. Bingham, H.G., Kemper, K.W., Fletcher, N.R.: Nucl. Phys. A**175**, 374 (1971)
34. Matsuki, S., Yamashita, S., Fukunaga, K., Nguyen, D.C., Fujiwara, N., Yanabu, T.: J. Phys. Soc. Japan **26**, 1344 (1969)
35. Stokstad, R.G.: Yale University, Report **52** (1972)
36. Cords, H., Din, G.U., Ivanovich, M., Robson, B.A.: Nucl. Phys. A**134** 561 (1968)
37. Hellström, J., Dallimore, P.J., Davidson, W.F.: Nucl. Phys. A**132**, 581 (1969)
38. Tamura, T.: Rev. Mod. Phys. **37**, 679 (1965)
39. Wolter, H.H.: CRC code, University of Munich (unpublished)
40. Harakeh, M.N., Popta, J. van, Saha, A., Siemssen, R.H.: Nucl. Phys. A**344**, 15 (1980)
41. Votava, H.J., Clegg, T.B., Ludwig, E.J., Thompson, W.J.: Nucl. Phys. A**204**, 529 (1973)
42. Satchler, G.R.: Nucl. Phys. A**100**, 497 (1967)
43. Bohr, A., Mottelson, B.R.: Nuclear structure II. Reading: W.A. Benjamin 1975
44. Skorka, S.J., Hertel, J., Retz-Schmidt, T.W.: Nucl. Data A**2**, 347 (1966)
45. Tamura, T., Low, K.S.: Comput. Phys. Commun. **8**, 349 (1974)
46. Jarczyk, L., Kamys, B., Rudy, Z., Strzałkowski, A., Styczen, B., Berg, G.P.A., Magiera, A., Meissburger, J., Oelert, W., Rossen, P. von, Römer, J.G.M., Kwasniewicz, E.: Z. Phys. A – Atoms and Nuclei **322**, 221 (1985)
47. Jarczyk, L., Kamys, B., Rudy, Z., Strzałkowski, A., Styczen, B., Berg, G.P.A., Magiera, A., Meissburger, J., Oelert, W., Rossen, P. von, Römer, J.G.M., Kwasniewicz, E.: Nucl. Phys. A**459**, 52 (1986)
48. Jarczyk, L., Kamys, B., Rudy, Z., Strzałkowski, A., Styczen, B., Berg, G.P.A., Magiera, A., Meissburger, J., Oelert, W., Rossen, P. von, Römer, J.G.M., Wolter, H.H., Kwasniewicz, E., Kisiel, J.: Nucl. Phys. A**448**, 1 (1986)
49. Messiah, A.: Quantum mechanics. Amsterdam: North-Holland 1966

A. Szczurek, K. Bodek, J. Krug, W. Lübcke, H. Rühl,
M. Steinke, M. Stephan, D. Kamke
Institut für Experimentalphysik I
Ruhr-Universität Bochum
D-4630 Bochum
Federal Republic of Germany

W. Hajdas, L. Jarczyk, B. Kamys, A. Strzałkowski
Institute of Physics
Jagellonian University
PL-30059 Cracow
Poland

E. Kwasniewicz
Institute of Physics
Silesian Technical University
PL-40010 Katowice
Poland